Impact of Industrial Robot Tool Mass on Regenerative Energy

Arturs Paugurs, Armands Senfelds, Leonids Ribickis
RIGA TECHNICAL UNIVERSITY
INSTITUTE OF INDUSTRIAL ELECTRONICS AND ELECTRICAL ENGINEERING
Azenes street 12/1
Riga, Latvia
+371 67089919
ieei@rtu.lv
http://ieei.rtu.lv/

Acknowledgments

This research is supported by Latvian National Research Programme project LATENERGI.

Keywords

«Regenerative power», «Robotics», «Industrial application»

Abstract

Recent research has shown great potential in energy efficiency optimization by harvesting regenerative energy of industrial robots. This paper presents further insight into how dependent regenerative energy is on the mass of the robot tool, as well as how the total regenerative energy is distributed between various robot links.

Introduction

Industrial robotics is one of the key factors for high productivity rates in today's automotive industry, thus having a significant impact on the total electrical energy consumption of the whole factory. An average high payload robot consumes 5.2 MWh annually only during the movement process [1]. Regenerative energy, which occurs due to rapid deceleration of the robot, can sum up to 20% of the abovementioned consumption energy (depending on the robot trajectory and movement parameters). In the state of the art robotic systems the regenerative energy is dissipated on braking resistors [2], which seems to be an outdated method, considering the possibilities of energy storage systems combined with bidirectional power converters, of which both have been researched and improved greatly in the recent years, driving the cost per kWh down and the efficiency up.

Several methods have been discussed and tested on harvesting the regenerative braking energy, thus increasing the overall energy efficiency of robotized production systems. These methods include the use of supercapacitor and battery energy storage systems, implementation of a DC supply microgrid and topology modifications of the robot's power supply unit [3]–[7]. However, not only hardware modifications could lead to improved energy efficiency, various software solutions have also been suggested where the robot movement trajectories and acceleration, deceleration patterns are recalculated as functions of energy consumption. These algorithms demonstrate an improvement in energy efficiency of robotic systems by up to 40% for specific robot cycle programs [8]–[10].

This study presents a better understanding on how the regenerative energy is distributed between robot joints and how dependent is its total amount on the mass of the robot tool.

Experimental Setup

Main components of the particular experimental setup are an industrial robot KUKA KR210, SIEMENS active frontend unit (AC/DC converter, 55 kW, 600 VDC output), DC power measurement device and a specific robot tool with variable mass.

To evaluate the impact of the robot tool mass on the total regenerative energy, a specific robot tool was designed with stackable iron blocks each having approximately 21 kg of mass. The maximum payload of the robot is 210 kg. Five experiments were logged with the following set points in load mass: 0 kg, 56 kg, 98 kg, 162 kg and 205 kg. KR210 has six links by default (A1..A6). Link numeration starts at the base of the robot and ends at the tool fixation plate, thus the variable load is attached to A6. A stack of seven blocks attached to the sixth link of the robot is depicted in Fig. 1, being the fourth set point of 162 kg.

Experimental data is obtained by electrical measurements of KUKA KR210 industrial robot's active infeed power whilst operating a specific robot movement program at maximum velocity. The program is designed to rotate each motor individually close to its angular limitations, a one second pause between each rotation is included for clear data separation at post-processing stage. Such program allows analyzing the impact of each robot link on the overall regenerative energy. Data post-processing was carried out in Matlab R2015a.

Excess energy occurs during rapid deceleration due to large kinetic energy and inertia. At such point the voltage of the conventional AC/AC power supply's DC bus increases and if it surpasses the value of the rectified AC supply voltage, a braking resistor is connected [1]. In this setup the robot's power supply is modified, excluding the built-in rectifier and the braking resistor and leaving the DC bus as the main power infeed point. The DC bus is then supplied externally from a stable 600V DC microgrid, which is generated by the SIEMENS active frontend unit, Fig. 2. In this way the excess, regenerative energy is fed back directly to the supply grid.

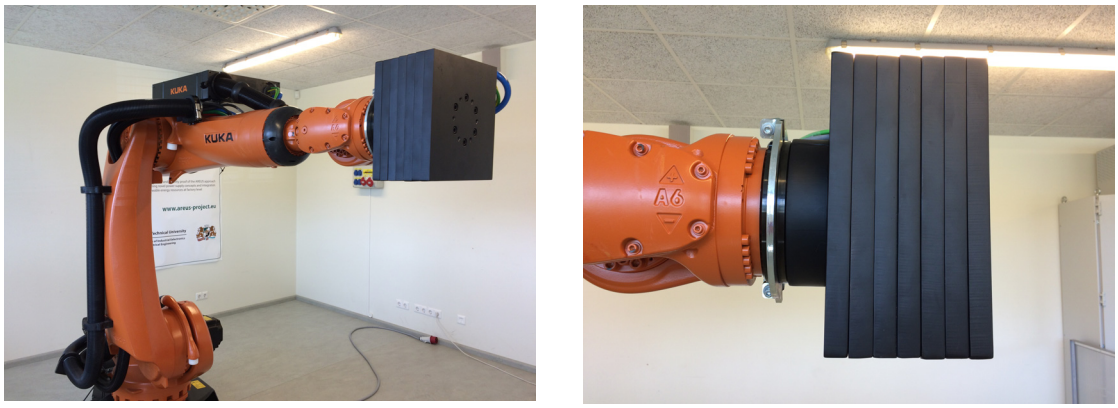

(a) (b)

Fig. 1. Whole industrial robot arm with load (a); variable load (b).

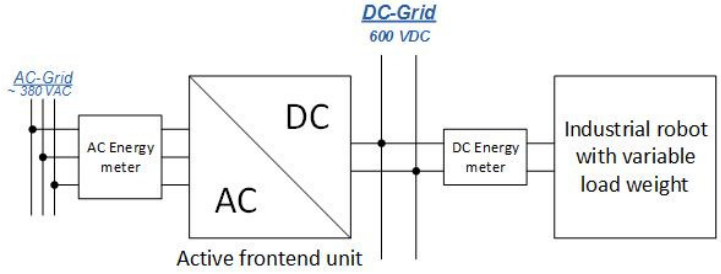

Fig. 2. Principal electrical schematic of the experimental setup.

Power Cycle Measurements

A power measurement of a single full cycle at two different load set points (0 kg and 205 kg) is depicted in Fig. 3. The dashed lines parallel to the Y-axis represent the beginning and the end of each motor's individual movement. For example, at t = 2 s, the largest motor located at the base of the robot (joint A1) starts rotating the robot arm from 0 to +120 angular degrees at maximum velocity. During the motion, only the motor of joint A1 is rotating. The positive power peak represents the maximum power demand due to acceleration, whilst the following negative power peak represents the regenerative power occurring due to rapid deceleration. When the 120 angular degree position is reached, the robot program reverses the motion and rotates the A1 joint from +120 to -120 angular degrees at maximum velocity (t ε [3.7; 6.3] s). Lastly, a third motion from -120 angular degrees to 0 degrees finishes the rotation of joint A1, bringing it to the home position where the motion began. In such manner each following joint (A2, A3, A4, A5 and A6) is individually rotated and its power demand and regeneration is measured and logged.

Comparison of the two power graphs in Fig. 3 shows that the larger mass of the tool significantly increases the consumed and regenerated power peaks of joints A1, A2 and A3, however, the opposite can be said about the regenerative power peaks of the smaller joints A4, A5 and A6, because the larger mass dampens the dynamics of their rotation, increasing the cycle execution time and decreasing the deceleration rate of these joints which leads to lower regenerative power peaks when comparing with the no-load (0 kg) measurement. The larger tool mass also stabilizes the consumption power profile of the smaller links (A4-A6). Motors of joints A1 and A2 have the highest power rating and their dynamics and cycle execution times are therefore less affected by the increase of mass of the tool.

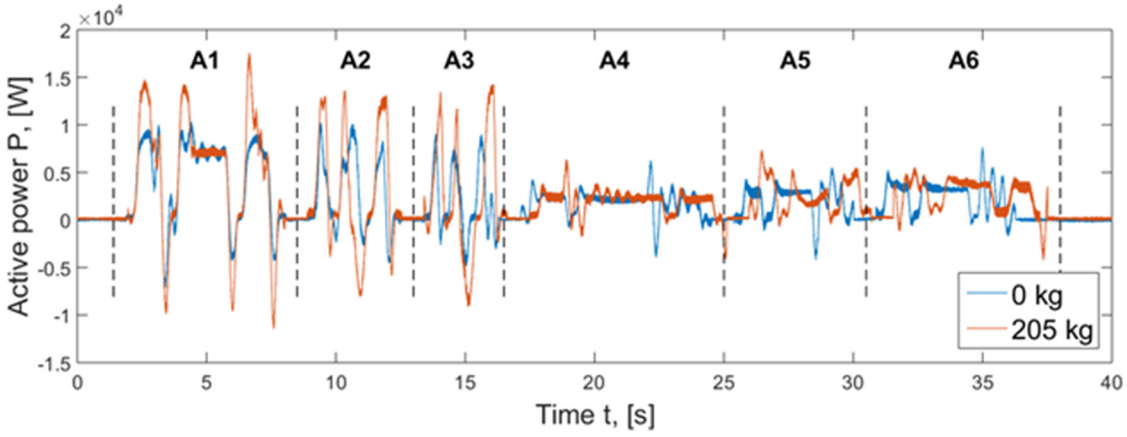

Fig. 3. Comparison of a full cycle power measurement at 0 kg and 205 kg load mass.

Energy Calculation and Analysis

The consumed and regenerated energies are calculated as integrals of measured electrical power graphs throughout the whole cycle (Eq. 1-2). The resulting data are presented in Fig. 4 for all tool mass set points. Intuitively, the total consumed and regenerated energies of the whole cycle increase with the tool mass, however, not with the same proportional coefficient. The rate of change for regenerative energy as a function of tool mass is higher than the rate of change for consumed energy, meaning that the relative regenerative energy (Eq. 3, Fig. 5) increases as well. In other words, the increase of the tool mass causes the regenerative energy to increase with a greater rate than the consumption energy. While the increase of tool mass from no load to 205 kg causes an increase in consumption energy by 23.00%, the regenerative energy increases by 94.60%.

$$E_{consumption} = \int_0^t Pdt; P \in [0;+\infty) \tag{1}$$

$$E_{recuperation} = \int_0^t Pdt; P \in (-\infty;0) \tag{2}$$

$$\varepsilon_{rec} = \frac{E_{recuperation}}{E_{consumption}} * 100\% \tag{3}$$

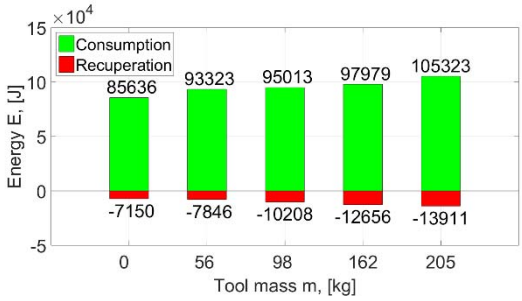

Fig. 4. Consumed and regenerated energy comparison in a single full cycle at different tool masses.

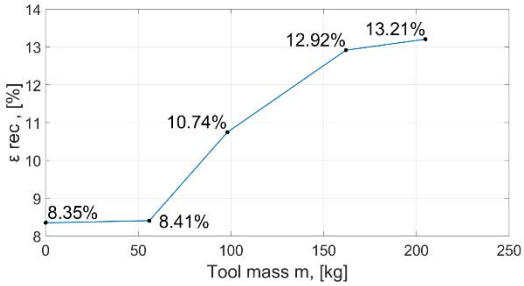

Fig. 5. Percentage of regenerative versus consumed energy as a function of the robot tool mass.

Each robot link's regenerative energy is analyzed by calculating its impact on the full cycle's regenerative energy (Eq. 5). To achieve this, the regenerative energy of each link is calculated separately in each respective time frame when the link is operating (Eq. 4). Time frames are depicted in Fig. 3 with the dashed lines parallel to y-axis.

Fig. 6 depicts the total regenerative energy distribution between each individual link throughout the whole cycle at different tool masses. The first three robot links (A1, A2 and A3) account for 80% to 91% of the full cycle's total regenerative energy, increasing their part proportionally with the tool mass. Vice versa occurs with the smaller, last three robot links (A4, A5 and A6). As the mass of the tool increases, these links account for a linearly decreasing part of the cycle's total regenerative energy – 20% to 9% - which is due to decreasing deceleration rate of links A4, A5 and A6 with increase of the tool mass.

$$E_{recA*} = \int_0^{A*} Pdt; P \in (-\infty;0) \tag{4}$$

$$\varepsilon_{recA*} = \frac{E_{recA*}}{E_{recuperation}} * 100\% \tag{5}$$

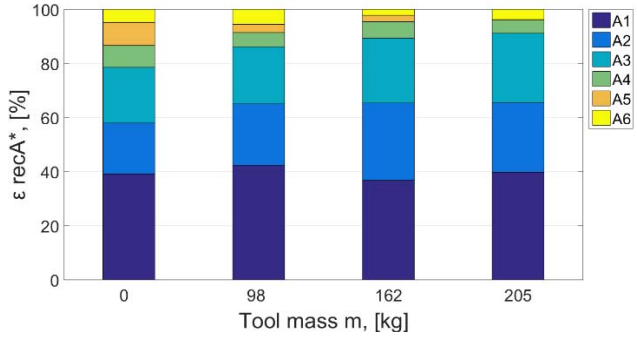

Fig. 6. Regenerative energy distribution between robot links at different robot tool masses.

Economical Aspects

While research and development towards a greener, more energy efficient manufacturing is mandatory, real hardware implementation in large scale manufacturing takes place only when the proposed solution is also economically viable (positive return on investment in a time period which is less than the amortization period of the installed system).

In the case of industrial robotics the calculation of the time period it would take for the return on investment to be positive largely depends on the robot's work cycle (thus, varying the power profile), work intensity (cycles per day), the total number of operating robots in the factory and the investment cost (hardware, installation costs) (Eq. 6).

$$t_{yrs} = \frac{HW_{cost}}{\sum_{k=1}^{k=Rcount} E_{rec(k)} * n_k * \eta_{HW} * e_{electricity}} \tag{6}$$

where:
t_{yrs} – the time period it takes for the investment to return (ROI = 0, in years).
HW_{cost} – the cost of the investment, for example, cost of the active frontend unit.
$E_{rec(k)}$ – the regenerative energy of a particular robot in a single robot cycle (in kWh).
n_k – the number of robot cycles in a year.
η_{HW} – efficiency of the hardware setup necessary for harvesting regenerative energy.
$e_{electricity}$ – the price of electrical energy per kWh.
R_{count} – the number of robots operating in the factory.

To obtain an optimal solution, the investment cost should be divided amongst as many industrial robots as possible. Article [11] addresses a similar issue of power dimensioning an active frontend unit in respect to the power profiles of various industrial robot cycles.

In order to effectively predict the economic aspects of integrating regenerative energy harvesting systems in robotized factories, time-related power profile analysis have to be performed, predicting the energy consumption levels at every given point during the production cycle. Such software planning solutions are proposed in [1].

Conclusion

An industrial robot KUKA KR210 with a modified power supply to enable the re-use of regenerative energy has been studied to better understand the distribution of the regenerative energy between various robot motors. A specific tool with variable masses has been designed to test the impact of the tool mass on the total regenerative energy.

An increase in the mass of the tool increases both the consumption and the regenerative energy, however, the regenerative energy increases with a higher rate in comparison to the consumption energy increase rate. The regenerative energy is 94.6% higher with a 205 kg tool when comparing to a no-load measurement (0 kg tool), whilst the consumption energy increases by 23% when comparing the same load set points.

Regarding the distribution of regenerative energy between various robot links, 80% to 91% of the whole cycle's regenerative energy, is caused by the braking of the first three motors (A1, A2 and A3) due to near-constant deceleration profile and higher motor power ratings. Last thee robot links (A4, A5 and A6) account for the remaining 20% to 9% of the total cycle's regenerative energy. Their impact on the total regenerative energy decreases due to lower deceleration rates caused by the increase of the tool mass.

In order to sufficiently plan the economic aspects of implementing regenerative energy harvesting systems in robotized factories, time-related power profile analysis have to be realized beforehand

for all robotized work cells. The potential economic benefits of such energy harvesting systems are highly dependent on the robot's work cycle, work intensity (cycles per day) and the total number of robots in the factory.

References

[1] D. Meike, "Increasing Energy Efficiency of Robotized Production Systems in Automobile Manufacturing," Riga Technical university, 2013.

[2] D. Meike and L. Ribickis, "Recuperated energy savings potential and approaches in industrial robotics," in *Automation Science and Engineering (CASE), 2011 IEEE Conference on*, 2011, pp. 299–303.

[3] M. Pellicciari, A. Avotins, K. Bengtsson, G. Berselli, N. Bey, B. Lennartson, and D. Meike, "AREUS - Innovative Hardware and Software for Sustainable Industrial Robotics," in *2015 IEEE International Conference on Automation Science and Engineering (CASE)*, 2015, pp. 1325–1332.

[4] K. Vitols, "Design considerations of a battery pack - DC grid interface converter," in *2015 IEEE 5th International Conference on Power Engineering, Energy and Electrical Drives (POWERENG)*, 2015, pp. 476–479.

[5] A. Senfelds, A. Avotins, L. Ribickis, and D. Meike, "Research and Demonstration of New DC Power Supply Concepts for EU Factories of Future at RTU," *Mater. Process. Technol. Riga Tech. Univ. Res.*, vol. 3, pp. 34–37, 2015.

[6] M. Vorobyov, "Research of power electronics converters for supercapacitor storage devices used in industrial systems," in *2015 IEEE 5th International Conference on Power Engineering, Energy and Electrical Drives (POWERENG)*, 2015, pp. 596–599.

[7] A. Senfelds, M. Vorobjovs, D. Meike, and O. Bormanis, "Power smoothing approach within industrial DC microgrid with supercapacitor storage for robotic manufacturing application," in *Automation Science and Engineering (CASE), 2015 IEEE International Conference on*, 2015, pp. 1333–1338.

[8] A. Fenucci, M. Indri, and F. Romanelli, "An off-line robot motion planning approach for the reduction of the energy consumption," in *2016 IEEE 21st International Conference on Emerging Technologies and Factory Automation (ETFA)*, 2016, pp. 1–8.

[9] M. Mahdavian, M. Shariat-Panahi, A. Yousefi-Koma, and A. Ghasemi-Toudeshki, "Optimal trajectory generation for energy consumption minimization and moving obstacle avoidance of a 4DOF robot arm," in *2015 3rd RSI International Conference on Robotics and Mechatronics (ICROM)*, 2015, pp. 353–358.

[10] A. Vergnano, C. Thorstensson, B. Lennartson, P. Falkman, M. Pellicciari, F. Leali, and S. Biller, "Modeling and Optimization of Energy Consumption in Cooperative Multi-Robot Systems," *IEEE Trans. Autom. Sci. Eng.*, vol. 9, no. 2, pp. 423–428, Apr. 2012.

[11] A. Senfelds, O. Bormanis, and A. Paugurs, "Analytical approach for industrial microgrid infeed peak power dimensioning," in *2016 57th International Scientific Conference on Power and Electrical Engineering of Riga Technical University (RTUCON)*, 2016, pp. 1–4.

This is a post-print of a paper published in Proceedings of the 2017 19th European Conference on Power Electronics and Applications (EPE '17 ECCE Europe), Warsaw, Poland, 11-14 September 2017 and is subject to IEEE copyright.
https://doi.org/10.23919/EPE17ECCEEurope.2017.8099185
ISBN 978-1-5386-0530-1
e-ISBN 978-90-75815-27-6.